Triphase Equilibria in Cellulose Nanocrystal Suspensions Containing Neutral and Charged Macromolecules

Stephanie Beck-Candanedo, David Viet, and Derek G. Gray*

Department of Chemistry, Pulp and Paper Research Centre, McGill University, Montréal, Québec H3A 2A7, Canada

Received February 26, 2007

ABSTRACT: The effect of added nonadsorbing macromolecules on the phase behavior of suspensions of electrostatically stabilized cellulose nanocrystals is examined. Triphasic isotropic−isotropic−nematic equilibria develop in cellulose nanocrystal suspensions to which a mixture of dextran and blue dextran is added. Phase diagrams for different combinations of uncharged dextran and anionically charged blue dextran are presented. The range of dextran concentrations at which the triphase equilibrium is produced is strongly influenced by the molecular weight of the blue dextran. Reentrant phenomena as well as regions of biphase coexistence are present in the phase diagrams. A threshold difference in charge density between two blue dextrans of varying degree of dye substitution is necessary for triphase equilibrium to occur at a given number density of each polymer species. Different repulsive electrostatic and attractive entropic forces may dominate at different concentrations of the dextrans, contributing to the rich phase behavior of these suspensions.

Introduction

The spontaneous phase separation of suspensions of rod- and platelike colloidal particles to give isotropic and nematic liquid crystalline phases is well-known and was reported as early as the 1920s.[1−8] The isotropic−nematic phase transition is purely entropic in nature: although the orientational entropy of the system decreases due to alignment of the rods in the nematic phase, this loss is more than offset by the increase in positional or translational entropy of the system. In other words, the free volume available to individual rods increases as the rods align. Such systems can display rich phase behavior; triphase isotropic−nematic−nematic (I−N−N) equilibria have been observed in suspensions of colloidal boehmite particles[5,9] as well as in suspensions of tunicate cellulose whiskers.[10]

It has been found that added particles or macromolecules of different shape can further enrich the phase separation behavior of suspensions of rodlike colloidal particles, leading to the formation of multiple phases.[11−14] Widening of the biphasic coexistence region by the addition of coiled macromolecules, and their preferential partitioning into the isotropic phase, was predicted theoretically by Flory, who stated that the addition of a coiled polymer increases the volume fraction of rodlike particles in the anisotropic phase.[15] Noninteracting macromolecules thus create attractive depletion forces between rodlike colloids, inducing phase separation in anisotropic suspensions.[16−18] Depletion-induced phase separation has been studied experimentally and theoretically for a variety of colloid−polymer systems.[5,14,19−22] The range of the depletion force depends on the size of the macromolecule, while the strength of the force depends on its concentration. Electrically charged macromolecules have been found to greatly increase the magnitude of the interaction.[17] The exact nature of the effect of attractive depletion forces on the phase behavior of suspensions of rodlike particles depends on the rod dimensions and polydispersity as well as the macromolecule concentration.[11−13]

Suspensions of electrostatically stabilized rodlike cellulose nanocrystals can be produced by acid hydrolysis of various types of cellulose, including bacterial, tunicate, cotton, and wood.[23−28] Within a narrow concentration range, these suspensions separate into isotropic and chiral nematic phases. Their phase separation behavior depends on the nanocrystal dimensions and surface charge density and on the ionic strength of the suspension and the nature of the counterions.[24,29−32] The addition of the polymer blue dextran 2000 has been shown to alter the phase separation behavior of aqueous suspensions of cotton cellulose nanocrystals by inducing the separation of an isotropic phase from completely anisotropic suspensions.[27] Blue dextran 2000 consists of a nonadsorbing glucose polymer containing ∼5% α-(1→3)-branching with a branched coil-like conformation.[33,34] It contains a sulfonated triazine dye, Cibacron blue 3G-A, covalently bound to random hydroxyl groups on the dextran chain.[35] However, later work has found that equivalent concentrations of *unmodified* dextran T-2000 do *not* induce phase separation in similar anisotropic suspensions.[36] The apparent inconsistency can be explained by the low ionic strength of the suspensions, which allows the electrostatic repulsion between the nanocrystals to screen the attractive depletion forces caused by the neutral dextran. An analogous phenomenon has been observed by Dogic et al. for suspensions of fd virus containing the neutral polymer dextran T-500.[21] Blue dextran contains anionic sulfonate groups as part of the dye molecules, which increase the ionic strength when added to the suspension, thereby increasing the critical concentration required for phase separation, and at higher concentrations, masking the inter-rod electrostatic repulsion sufficiently to allow depletion attractions to dominate.[36,37]

Preferential partitioning of blue dextran into the isotropic phase of cellulose nanocrystal suspensions has been measured for biphasic and initially anisotropic suspensions, and a widening of the isotropic−nematic (I−N) coexistence region was observed.[27] Greater partitioning occurred at higher blue dextran concentrations.[38] In an attempt to measure the effect of the concentration of only the dextran portion on the partitioning of blue dextran between the isotropic and chiral nematic phases, increasing amounts of unmodified dextran were added to samples of biphasic cellulose suspension containing a fixed concentration of blue dextran. However, after mixing and

* To whom correspondence should be addressed: e-mail derek.gray@mcgill.ca; Tel 514-398-6182.

10.1021/ma0704818 CCC: $37.00
Published on Web 03/31/2007

Table 1. Molecular Weights, Polydispersities, and Radii of Gyration of Dextrans Used[42−44]

dextran	$\bar{M}_w$ (kDa)	$\bar{M}_n$ (kDa)	Ip	R_g (nm)
T-2000	2000			34.0
T-500	532	183	2.91	19.8
T-110	106	80.9	1.31	9.7

equilibration, the samples unexpectedly displayed three phases: an upper isotropic (I_1) phase into which the blue dextran appears to partition preferentially, a middle isotropic (I_2) phase, and a lower chiral nematic (N) phase.

Triphase isotropic−isotropic−nematic (I−I−N) and isotropic−nematic−nematic (I−N−N) equilibria have been predicted theoretically for rodlike colloid and flexible polymer systems[11,39] and have been observed in sterically stabilized boehmite rod suspensions, both with[5] and without [9] added polymer. To our knowledge, triphase I−I−N equilibria in cellulose nanocrystal suspensions have not been reported in the literature. The present article examines the phase behavior for various dextran/blue dextran/cellulose nanocrystal systems and investigates the effect of variables such as dextran molecular weight and cellulose concentration on the appearance of the associated phase diagrams.

It should be noted that although the liquid crystalline phase of the cellulose suspensions is chiral nematic, the term nematic (N) will be used; the free energy difference between nematic and chiral nematic phases is much smaller than that between isotropic and anisotropic (whether nematic or chiral nematic).[40] This allows results for the chiral nematic phase to be compared with theories developed for nematic phases.

Experimental Methods

Chemicals. Dextrans T-110, T-500, and T-2000 (see Table 1) and blue dextran 2000 ($\bar{M}_w \approx 2\,000\,000$ with 0.1 mmol of Reactive Blue 2 dye per gram of dextran bonded randomly via an ether linkage to the polymer backbone[41]) were purchased from Pharmacia Fine Chemicals. Cibacron blue 3G-A (55% dye content) was purchased from Sigma-Aldrich and used without further purification. Whatman ashless cotton cellulose powder was purchased from Cole-Parmer. Sulfuric acid (95−98%) for hydrolysis was purchased from Fisher Scientific. Sodium hydroxide, sodium chloride, and sulfuric acid volumetric standards for conductometric titration were purchased from Aldrich. All water used was purified with a Millipore Milli-Q purification system.

Cellulose Nanocrystal Suspensions. Cellulose nanocrystal suspensions were prepared as described in a previous publication.[36] Conductometric titration was used to determine the surface charge density of the cellulose nanocrystals associated with surface sulfate ester groups. The suspension was then concentrated to 8.7 wt % by evaporation under ambient conditions. The average nanocrystal length measured by tapping-mode atomic force microscopy (TM-AFM) was 200 ± 15 nm.

Blue Dextrans. Blue dextrans of various molecular weights and ligand densities (Table 2) were prepared and characterized as described in a previous publication.[36] Blue dextran samples are denoted by their molecular weight followed by a subscript number indicating the degree of dye substitution (DS) per anhydroglucose repeat unit (AGU). According to convention, commercially available blue dextran 2000 purchased from Pharmacia will be referred to as "blue dextran 2000", except where necessary for clarity.

Preparation of Cellulose−Dextran Suspensions. Samples were prepared by adding solid dextran to aliquots of concentrated cellulose nanocrystal suspension and vortexing until homogeneous dispersion was achieved. Suspensions were allowed to equilibrate and monitored over a period of at least 2 weeks. The phase volume fractions were determined by measuring the heights of the anisotropic and isotropic phases in each vial.

Table 2. Preparation Conditions and Ligand Densities of Blue Dextrans

blue dextran[a]	reaction time (h)	initial dye−dextran ratio (mol:mol)	$[Na_2CO_3]$ (M)	ligand density (DS per AGU, 10^{-4})
2000_{16}	21.5	300	0.010	16
2000_{18}	45	350	0.125	18
2000_{36}	96.5	300	0.010	36
2000_{56}	144.5	300	0.010	56
2000_{161}	*b*	*b*	*b*	161
500_{49}	48	300	0.010	49
110_{129}	120	300	0.45	129

[a] Subscripts indicate dye ligand density. [b] Commercially available blue dextran 2000 (Pharmacia Fine Chemicals).

Table 3. Hydrodynamic Radii of Unmodified Dextrans and Blue Dextrans in 0.200 M NaCl(aq) Obtained by Dynamic Light Scattering

dextran[a]	R_H (nm)
dextran T-2000	37.7 ± 0.8
blue dextran 2000_{161}	40.2 ± 0.8
dextran T-500	17.8 ± 0.3
blue dextran 500_{11} [b]	18.4 ± 0.7
dextran T-110	7.7 ± 1.2
blue dextran 110_{22}[b]	30.7 ± 3.1

[a] Subscripts indicate dye ligand density (DS per AGU, 10^{-4}). [b] N.B. DLS performed on different samples of blue dextrans 500 and 110 than those used in phase diagrams due to limited sample quantities.

The number density, C_i, of the blue dextran and dextran molecules in the samples was calculated using the equation

$$C_i = \frac{N_i}{V_{tot}} = \frac{N_a m_i}{V_{tot} M_i}$$

where N_i is the number of molecules of species i, V_{tot} is the volume of the sample, N_a is Avogadro's number, m_i is the mass of species i, and M_i is the molar mass of species i. It should be noted that while number-average molecular weight, $\bar{M}_n$, should be used in the formula for number density, the molecular weights given for the dextrans are weight-average, $\bar{M}_w$ (supplier's data).

Characterization Methods. Photomicrographs of the three phases were taken using a polarized light microscope (Nikon Microphot-FXA). Pitch measurements were performed on microscope images of the chiral nematic (N) phase.

The dye content of the dextran−dye conjugates was determined using UV−vis spectroscopy (Varian Cary 300 Bio spectrophotometer). A calibration curve was obtained from solutions of commercially available blue dextran 2000, and adherence to the Beer−Lambert law was established. The ligand density was estimated from absorbance measurements at 609 nm for solutions of the dextran−dye conjugates and calculated in terms of the degree of substitution (DS) per anhydroglucose (AGU) repeat unit (see Table 2).

To measure the partitioning of blue dextran among the phases of the suspensions, aliquots of each phase were carefully removed and diluted to minimize scattering by the cellulose nanocrystals. Concentrations of blue dextran 2000 in each phase were measured spectrophotometrically using dextran-free cellulose nanocrystal suspensions as the reference. Partition coefficients $K = d_I/d_N$ were calculated by dividing the absorbance due to blue dextran in the isotropic phases by the absorbance of blue dextran in the anisotropic phase.[45]

The hydrodynamic radii of the blue dextran 2000 and dextran T-2000 (Table 3) were calculated using dynamic light scattering (DLS). Solutions of dextran and blue dextran (0.2−1.0 g/L) were prepared in 0.200 M NaCl(aq). The solutions and solvents were clarified by filtration through a nylon filter of pore size 0.2 μm (Millipore); samples were filtered directly into the light scattering cells. Light scattering measurements were made at 21−22 °C on a Brookhaven Research BI-200SM laser light scattering goniometer

Figure 1. Vials of triphase I_1-I_2-N equilibrium in cellulose nanocrystal suspension (8.7 wt %) containing commercial blue dextran 2000 (from left to right, 0.45 to 2.50 $\times$ 10^{-6} nm^{-3}) and dextran T-2000 (5.3 $\times$ 10^{-6} nm^{-3}). The preferential partitioning of blue dextran into the I_1 phase is evident. The volume fraction of the I_1 phase increases from left to right as more blue dextran 2000 is added.

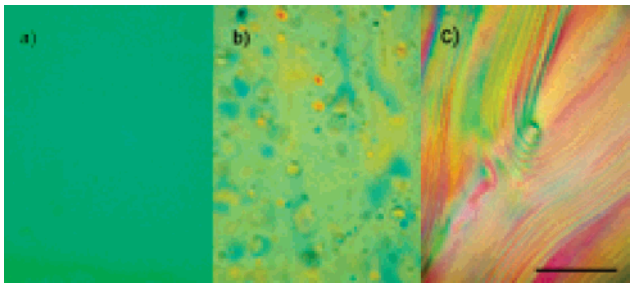

Figure 2. Photomicrographs of (a) I_1, (b) I_2, and (c) N phases. Taken at 10$\times$ magnification between crossed polars with 530 nm full-wave retardation plate. Streaks and droplets are visible in (b) due to ordering at the surface of the glass capillary. Characteristic chiral nematic fingerprint texture with ~38 μm pitch is visible in (c). Scale bar = 250 μm.

and BI-2030AT digital correlator, using a polarized incident beam of wavelength 632.8 nm from a He−Ne laser (35 mW total power). DLS measurements were made at a 90° angle with sample times of 20 μs over a duration of 30 s.

Results and Discussion

Triphase Equilibrium. When neutral dextran and polyelectrolytic blue dextran are added to an 8.7 wt % biphasic cellulose nanocrystal suspension ($\phi_{aniso} = 0.40$), a three-phase coexistence develops (Figure 1). The appearance of the phases when viewed between partially crossed polars and using polarized light microscopy (Figure 2) suggests that the new phase is a dilute isotropic phase. No birefringence or "order" is visible in the upper phase, while the birefringence seen in the middle phase can be explained by a thin layer of nematic ordering on the surface of the glass (cf. ref 5). In addition, the upper and middle phases mix very easily upon gentle shaking, while the lower phase is barely disturbed. The three phases in equilibrium are designated, from top to bottom, as I_1, I_2, and N.

Theoretical predictions and experimental evidence for dispersions of sterically stabilized boehmite rods and polystyrene in orthodichlorobenzene, a comparable system, suggest that the three phases in equilibrium are, from top to bottom, dilute isotropic (I_1), concentrated isotropic (I_2), and chiral nematic (N).[5,9,11] The terms "dilute" and "concentrated" refer to the relative cellulose nanocrystal concentrations of the phases. A diagram of the dependence of the type of phase behavior of

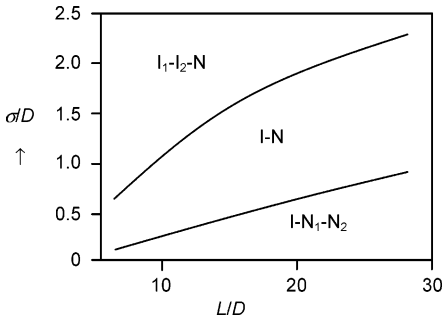

Figure 3. Type of phase behavior shown by mixtures of rodlike colloids and flexible polymers as a function of the geometrical parameters L/D and σ/D.[5,11] L is the rod length, D is the rod diameter and σ is the diameter of the polymer coil. "I_1-I_2-N" indicates a phase diagram with two isotropic phases and a nematic phase. Figure adapted from ref 11.

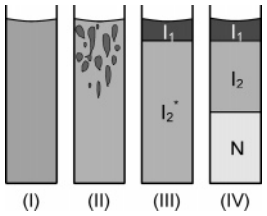

Figure 4. Schematic representation of the evolution of phase separation as typically observed in the three-phase coexistence region: (I) t_0, initially uniform sample; (II) t = 10−20 min, droplets of I_1 phase moving upward (bicontinuous structure of I_1 and I_2* phases); (III) t = 1−3 h, well-defined I_1 phase with metastable I_2* phase; (IV) t = 48−96 h, final I_1-I_2-N coexistence.

rodlike colloid and flexible polymer mixtures on the size parameters of the components is shown in Figure 3. The theory is not limited to the second virial level and is therefore not restricted to very long rods and very low polymer concentrations.[11] When blue dextran 2000 and dextran T-2000 are used as the polymers, the parameters for our system are $L \approx 200$ nm, $D = 5-10$ nm, and $\sigma \approx R_g = 34$ nm. Thus, $L/D \approx 20-40$ and $\sigma/D \approx 6.8-13.6$. For blue dextran 500_{49} and dextran T-500 ($R_g = 19.8$ nm), we obtain $\sigma/D \approx 4.0-8.0$. Our systems clearly lie in the I_1-I_2-N region of the diagram. However, because the colloidal cellulose rods are electrostatically rather than sterically stabilized, their interactions will be complicated by repulsion between the charged species, so the diagram may not correspond quantitatively to our system. Additionally, the coil-to-polymer diameter ratio in our system is larger than those shown in Figure 3; this parameter also influences the phase behavior, as the range of the depletion attraction is determined by the ratio of the radii of colloidal and polymer spheres.[5]

In cellulose nanocrystal suspensions, mixtures of commercial blue dextran 2000 and dextran T-2000 induce triphase equilibria at number densities of around 4 $\times$ 10^{-7} and 1 $\times$ 10^{-6} nm^{-3}, respectively (see Figure 5). Medium-molecular-weight dextrans (blue dextran 500_{49} and dextran T-500) induce triphase equilibria, but at such high dextran number densities that the samples are very viscous (equilibration times on the order of days to weeks), limiting the number of data points in the high-concentration regimes. When mixtures of low-molecular-weight dextrans (blue dextran 110_{129} and dextran T-110) are used, no third phase is seen at similar number densities to those used for the dextrans 2000; before reaching concentrations favoring triphase equilibrium, the increasing viscosity and time required for macroscopic phase separation render the experiments impractical.

Phase Separation. The kinetics of I_1 phase separation differ from those of the $N-I_2$ equilibration. To measure the phase

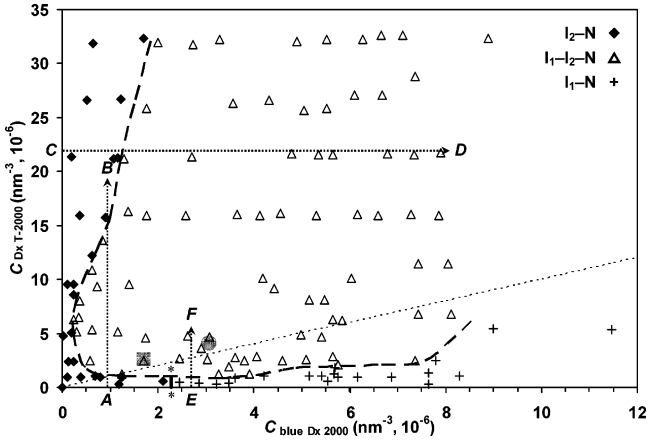

Figure 5. Phase diagram for 8.7 wt % cellulose nanocrystal suspension containing blue dextran 2000 and dextran T-2000. Dotted line indicates equal number densities of dextran and blue dextran. The boundaries between the regions of the phase diagram are intended as a guide to the eye. Some of the over 200 data points have been omitted for clarity. Compositions of phases along the lettered arrows are shown in Figures 6−8. Shaded areas correspond to mixtures of blue dextrans of different DS; see text.

separation kinetics, an 8.7 wt % cellulose nanocrystal suspension containing blue dextran and unmodified dextran is vortexed until homogeneity is achieved (t_0), and the initially uniform sample is allowed to equilibrate ($t > t_0$). As shown in Figure 4, the I_1 phase generally separates out within hours (macroscopic droplets moving upward are visible), followed by the N and I_2 phases within 2−4 days, except at high dextran/blue dextran concentrations, when equilibration can take much longer (weeks to months) due to the high suspension viscosity. Our observations are similar to those made by Poon et al. and Renth et al. for hard-sphere-like sterically stabilized poly(methyl methacrylate) (PMMA) particles and linear polystyrene (PS) in *cis*-decalin.[46−48] The rapidity of the demixing of our I_1 phase suggests that the phase separation proceeds by a spinodal decomposition mechanism.[46]

Dextran Partitioning. Blue dextran is known to partition preferentially into the isotropic phase of an I−N biphasic cellulose nanocrystal suspension.[27] UV−vis spectroscopy was used to obtain partition coefficients for blue dextran in the three phases of one sample in the blue dextran 2000 + dextran T-2000 system. The coefficients for partitioning of blue dextran between the N−I_1 and N−I_2 phases were $K_{NI_1} = 34.5$ and $K_{NI_2} = 4.1$, respectively. Partitioning between the two isotropic phases ($K_{I_2I_1} \approx 8.5$) is stronger even than partitioning between the N and I_2 phases, indicating a marked preference of the blue dextran for the dilute isotropic phase.

The exclusion of blue dextran 2000 from the nematic phase is not complete (nonzero absorbance at $\lambda_{\max CB} = 609$ nm is observed for the nematic phase). Some blue dextran coils are therefore able to be incorporated into the ordered structure of the liquid crystalline nematic phase. This behavior has been seen by Adams et al. for the lamellar phase of bacteriophage fd virus and polystyrene[14] as well as by Edgar and Gray for blue dextran 2000 and cellulose nanocrystals, where the lower nematic phase showed distorted fingerprint textures and many disclinations relative to a dextran-free nematic phase.[27]

Phase Diagram. When a combination of dextran and blue dextran of high molecular weight is added to a biphasic I−N cellulose suspension, I_1−I_2−N coexistence develops. Figure 5 presents a detailed diagram of the phase behavior of cellulose nanocrystal suspensions containing commercial blue dextran 2000 and dextran T-2000. All measurements were taken after several weeks to allow sufficient time for equilibration of the more viscous samples. The phase diagram is restricted to number densities below 4×10^{-5} nm^{-3} dextran and 1.2×10^{-5} nm^{-3} blue dextran; above these limits, the viscosity of the samples renders the phase separation kinetics impractical.

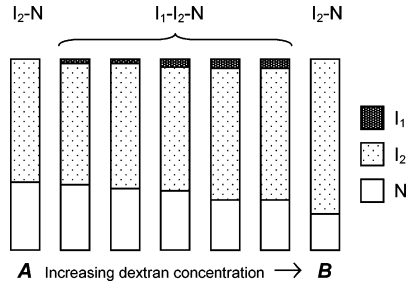

Figure 6. Example of reentrant I_2−N → I_1−I_2−N → I_2−N phase behavior for 8.7 wt % cellulose nanocrystal suspension containing 8.2×10^{-7} nm^{-3} blue dextran 2000 and dextran T-2000 increasing from 0 to 2.0×10^{-5} nm^{-3} (concentrations correspond to arrow AB in Figure 5). As dextran T-2000 is added, the N phase volume fraction decreases and the I_2 phase volume fraction increases; the I_1 phase increases and then decreases in volume fraction before disappearing.

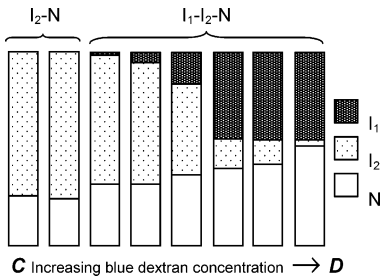

Figure 7. Example of phase behavior for 8.7 wt % cellulose nanocrystal suspension with dextran T-2000 number density = 2.2×10^{-5} nm^{-3} and increasing blue dextran 2000 number density (concentrations correspond to arrow CD in Figure 5). The I_1−N coexistence is not shown.

For the ranges of dextran concentration used, the majority of the samples are triphasic. At low blue dextran concentrations, the suspensions remain I_2−N biphasic, while at higher blue dextran concentrations and low dextran concentrations, the suspensions become I_1−N biphasic. The boundary between the I_2−N and I_1−N coexistences (line indicated by * in Figure 5) is somewhat arbitrary, as no distinct transition was seen when adding blue dextran 2000 at low dextran T-2000 concentration. The designations I_2−N and I_1−N were assigned according to the relative volume fractions of the three phases upon reaching triphase equilibrium. For example, in Figure 6, the I_2 phase dominates the triphasic sample, so the initial and final biphasic samples are designated I_2−N; in contrast, the I_1 phase dominates the initial triphasic sample in Figure 8. Using this nomenclature, there will be a continuous change from I_2−N to I_1−N coexistence, rather than a sharp boundary.

Smaller amounts of polyelectrolytic blue dextran are necessary for the formation of the I_1 phase compared to undyed dextran. The dotted line in Figure 5 indicates equal number densities of blue and unmodified dextran 2000; the I_1−I_2−N and I_2−N equilibria mostly lie above the dotted line, while I_1−N equilibrium lies below the line.

An interesting feature of the phase diagram is the reentrant I_2−N → I_1−I_2−N → I_2−N phase behavior observed with increasing plain dextran concentration at low blue dextran concentrations (arrow AB in Figure 5). As dextran T-2000 is added to a suspension containing a given concentration of blue dextran 2000, the I_1 phase appears, increases in volume fraction,

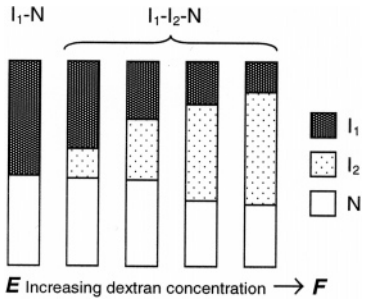

Figure 8. Example of phase behavior for 8.7 wt % cellulose nanocrystal suspension at blue dextran 2000 number density = 2.7×10^{-6} nm^{-3} and increasing dextran T-2000 number density (concentrations correspond to arrow EF in Figure 5).

then decreases in volume fraction, and disappears (Figure 6). At the same time, the N phase decreases in volume fraction. Reentrant phase behavior has been observed in both thermotropic and lyotropic molecular liquid crystal systems.[49] However, it is not well understood, particularly for lyotropic liquid crystalline systems. The only lyotropic liquid crystalline system in which the phenomenon is observed is the potassium laurate/decanol/water system,[50] for which reentrant isotropic−discotic nematic phase transition was first documented by Yu and Saupe in 1980.[51] It should be noted that the "reentrant" biphasic I_2-N suspension has a smaller volume fraction of N phase than the initial biphasic sample, likely due to the higher concentration of anionic blue dextran.

Effect of Increasing Blue Dextran Concentration. Adding blue dextran 2000 to a biphasic I_2-N cellulose suspension containing a fixed quantity of undyed dextran T-2000 results in the development of the triphase I_1-I_2-N equilibrium, followed by the I_1-N equilibrium (Figure 7). Following the formation of the I_1 phase, the I_2 phase continues to diminish, eventually disappearing, while the I_1 phase increases in volume fraction. The N phase also increases in volume fraction. The I_1 phase volume fraction continues to increase when the I_1-N coexistence has been established.

As shown in Figure 5, the blue dextran concentration is fairly low at the onset of triphase equilibrium. The increase in I_2 phase volume fraction prior to this probably results from a combination of (1) the higher ionic strength due to the charged dye ligands on the blue dextran and the resulting increase in critical cellulose concentration required for phase separation and (2) destabilizing attractive depletion forces, both of which would tend to favor the formation of I_2 phase.

Once the I_1 phase appears, the decrease in volume fraction of the I_2 phase with increasing blue dextran concentration indicates that the I_1 phase is more favorable than the I_2 phase. Increasing blue dextran appears to favor demixing to give the I_1 phase: The stability of the $N-I_1$ equilibrium is enhanced relative to that of the $N-I_2$ equilibrium as the blue dextran concentration increases. The observed decrease in N phase volume fraction as the blue dextran number density continues to increase is most likely due to the increasing ionic strength due to the dye ligands.

Effect of Increasing Dextran Concentration. At blue dextran concentrations favoring reentrant phase behavior, adding dextran T-2000 to a mixture of cellulose nanocrystal suspension and blue dextran 2000 causes the I_1 phase to appear, increase in volume fraction, then decrease, and disappear, while the I_2 phase increases slightly in volume fraction and the volume fraction of the N phase decreases somewhat overall.

At blue dextran concentrations lying in the $I_1-N \rightarrow I_1-I_2-N$ region of the phase diagram (i.e., at $C_{\text{blue Dx}} \geq 2 \times 10^{-6}$ nm^{-3}), increasing the dextran concentration leads to a decrease in the volume fraction of the I_1 phase and increasing formation of the I_2 phase. The volume fraction of the N phase also decreases, as would be expected due to depletion-induced phase separation. Figure 8 shows the phase behavior of samples with $C_{\text{blue Dx}} = 2.7 \times 10^{-6}$ nm^{-3}. Because the volume fraction of I_1 phase decreases with increasing dextran concentration, it is likely that the I_2-N coexistence region would be reached at higher dextran concentrations if sample viscosity permitted.

Increasing the concentration of the electrostatically neutral dextran should theoretically increase the magnitude of the depletion attraction.[17] However, the presence of polyelectrolytic blue dextran may complicate the situation even though its number density is held constant for these experiments. Phase behavior in the reentrant $I_2-N \rightarrow I_1-I_2-N \rightarrow I_2-N$ region of the phase diagram may be an example of this interplay between the attractive depletion and repulsive electrostatic forces.

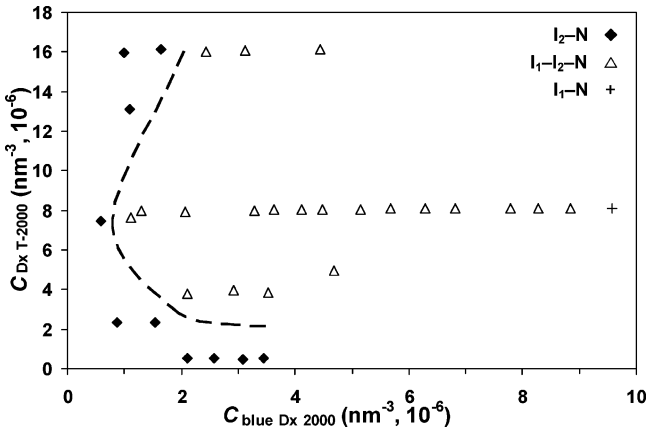

Figure 9. Partial phase diagram for dilute biphasic (6.3 wt %; $\phi_{\text{aniso}} = 0.29$) cellulose suspension. The boundary between the regions of the phase diagram is intended as a guide to the eye.

Table 4. Effect of Cellulose Nanocrystal Concentration on Dextran and Cellulose Number Densities Required To Obtain Triphase Equilibrium

series	[cellulose] (wt %)	phases	$C_{\text{blueDx}}/C_{\text{Dx}}$	$C_{\text{Dxtot}}/C_{\text{cell}}$
I	2.0	isotropic	0.3	6.5
	2.5	isotropic	0.3	5.0
	3.0	isotropic	0.3	4.2
	3.5	isotropic	0.3	4.3
	4.0	isotropic	0.3	3.0
	6.0	triphasic I_1-I_2-N	0.3	2.1
II	2.0	biphasic I−N	0.5	15.8
	2.5	triphasic I_1-I_2-N	0.5	12.8
	3.0	triphasic I_1-I_2-N	0.5	10.9
	3.5	triphasic I_1-I_2-N	0.5	9.2
	4.0	triphasic I_1-I_2-N	0.5	7.9

Effect of Cellulose Nanocrystal Concentration. A series of samples were prepared using a cellulose suspension of lower concentration (6.3 wt % cellulose; $\phi_{\text{aniso}} = 0.29$). The phase diagram in Figure 9 shows that, in comparison with Figure 5, more blue dextran 2000 is needed to obtain triphase equilibrium when the suspension is more dilute.

In order to determine whether triphase equilibrium was attainable starting from a monophasic suspension, two series of dilute (completely isotropic) suspensions with increasing cellulose concentration were prepared, and dextran T-2000 and blue dextran 2000 were added (Table 4). The dextran concentrations were comparable to those used in the 8.7 wt % cellulose suspensions, as were the blue-to-plain dextran ratios used (0.3 and 0.5 in series I and II, respectively). At the dextran concentrations used in the first series, it can be seen that triphase

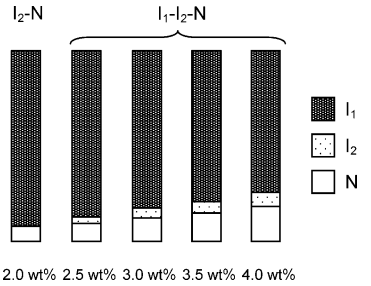

Figure 10. Relative volume fractions of the phases obtained when blue dextran 2000 and dextran T-2000 ($C_{\text{blue Dx}} = 6.0 \times 10^{-6}$ nm^{-3} and $C_{\text{Dx}} = 1.2 \times 10^{-5}$ nm^{-3}) were added to dilute cellulose suspensions (series II in Table 4).

equilibrium was not obtained until the cellulose concentration reached 6 wt %. The second series showed triphase equilibrium in all but the most dilute cellulose suspension (Figure 10). In both series, it is evident that the number density ratio of total dextran to cellulose necessary for triphase equilibrium increases with decreasing cellulose concentration.

The initial cellulose nanocrystal suspension evidently does not have to be biphasic for triphase equilibria to occur, since suspensions at cellulose concentrations well below the I−N transition show triphase equilibria upon addition of dextran and blue dextran. This is similar to experimental evidence found by Koenderink et al., who observed a depletion-induced phase transition in a mixture of colloidal silica spheres and silica-coated boehmite rods at rod concentrations well below the isotropic−nematic transition.[52] Anisotropic rods give rise to larger attractions than equivalent volume fractions of spheres because of the much higher rod number density,[53] which may explain the ability of the dilute suspensions to phase separate. As the cellulose suspension becomes more dilute, however, a higher total dextran-to-cellulose ratio is required to obtain three-phase coexistence (Table 4).

It is known that electrostatic interactions stabilize mixtures of charged colloids and polymers against depletion-induced phase separation and that increasing the range of the electrostatic interactions enhances the stabilization.[54,55] The more dilute cellulose suspensions contain fewer total surface sulfate groups and their associated counterions in solution, and therefore have lower ionic strengths, which reduces the screening of electrostatic interactions between charged macromolecules. This has a weakening effect on the (neutral or charged) polymer depletion-induced attraction between cellulose nanocrystals, ultimately resulting in increased stability toward demixing. In addition, since the nanocrystals themselves are farther apart in dilute suspensions, higher concentrations of macromolecular depletant would be needed to increase the strength of the depletion attraction to the point where phase separation occurs. (We can also predict that molecular weight effects will be stronger in the dilute suspensions because the range of depletion attraction is dependent on this variable; if the nanocrystals are farther apart, the equilibrium will be more sensitive to the range of the attraction force.)

Effect of Dextran Molecular Weight. Phase diagrams for mixtures of medium molecular weight dextrans are shown in Figure 11. The triphase coexistence region for mixtures of blue dextran 500_{49} and dextran T-500 (Figure 11a) is shifted to higher number densities of both blue dextran and plain dextran relative to mixtures of blue dextran 2000 and dextran T-2000 (Figure 5). In contrast, mixtures of blue dextran 2000 and dextran T-500 (Figure 11b) are shifted only slightly toward higher number densities of plain dextran. Finally, mixtures of blue dextran 500_{49}

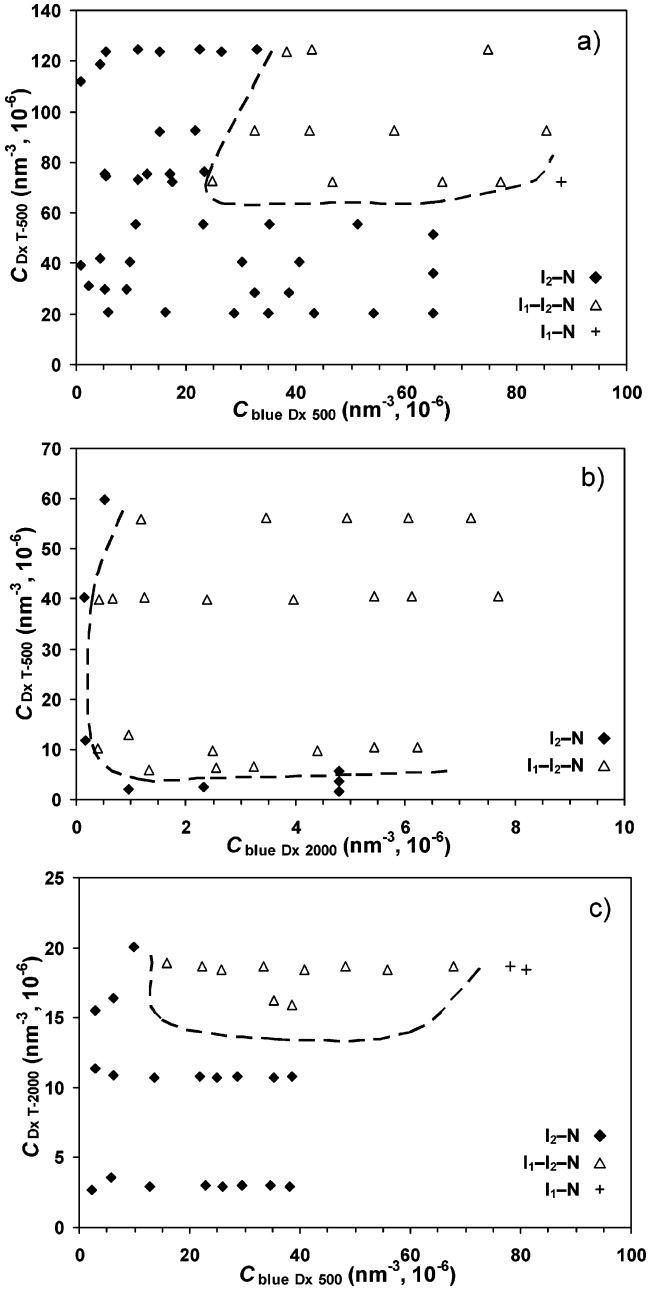

Figure 11. Phase diagrams for 8.7 wt % cellulose nanocrystal suspension containing (a) blue dextran 500_{49} and dextran T-500; (b) blue dextran 2000 and dextran T-500; and (c) blue dextran 500_{49} and dextran T-2000. The boundaries between the regions of the phase diagram are intended as a guide to the eye. Note: the phase diagrams are not on identical scales.

and plain dextran T-2000 are shifted to higher number densities for both types of dextran (Figure 11c). Mixtures of blue dextran 2000 and dextran T-110 also give triphase equilibria at relatively high dextran number densities, but mixtures of blue dextran 110_{129} and dextran T-2000 do not. The concentration ranges at which triphase equilibrium occurs for blue dextran 2000 + either dextran T-2000 or T-500 more or less overlap. These results suggest that the molecular weight of the polyelectrolytic blue dextran dominates the phase behavior of such mixtures, determining when triphase equilibrium develops.

For medium molecular weight blue dextran 500_{49}, the size of the unmodified dextran also influences the phase diagram to a large extent; much more dextran T-500 than dextran T-2000 is needed for triphase equilibrium (cf. parts a and c of Figure 11). The size of the unmodified dextrans has a much smaller

effect on the phase behavior of the mixture when high molecular weight blue dextran 2000 is used, increasing only slightly the number density of lower molecular weight plain dextran required for triphase coexistence (cf. Figures 5 and 11b). The phase diagrams in Figure 11 are not complete, owing to the difficulty of working at the high sample viscosities caused by the necessary higher dextran concentrations.

It has been found that dextrans of medium and high molecular weights (500−2000 kDa) induce formation of the I_1 phase in cotton cellulose nanocrystal suspensions, while dextrans of low molecular weight (110 kDa, results not shown) do not induce formation of the I_1 phase in the concentration range examined. Higher concentrations of the smaller dextrans are required, as the range of depletion forces depends on the macromolecule size.[17] These differences are reflected in Figure 11.

Effect of Blue Dextran Charge Density. Blue dextrans 2000 having low ligand densities (blue Dx's 2000_{16}, 2000_{18}, 2000_{36}, and 2000_{56}) were used instead of unmodified dextran T-2000 in mixtures with highly substituted commercial blue dextran 2000_{161} and 8.7 wt % cellulose nanocrystal suspension at two different number density combinations. For comparison with the blue Dx 2000_{161}/Dx T-2000 system, the number density combinations are indicated by shaded areas in Figure 5. At dextran concentrations corresponding to the shaded square, triphase equilibrium was observed only when blue dextran 2000_{16} was used, the other blue dextrans with higher degrees of substitution all yielding biphasic I−N suspensions. However, at higher blue dextran/dextran concentrations corresponding to the shaded circle in Figure 5, all the samples showed triphase equilibrium. It can be concluded that a minimum difference in charge density between the two blue dextrans is necessary for triphase equilibrium to occur at a given number density of each polymer species. In other words, the triphase coexistence regions of the phase diagrams for combinations of blue dextrans shift to higher concentrations of each macromolecular component as the difference in their charge density diminishes. This phenomenon may also partially explain the shift to higher concentrations between the phase diagrams when unmodified dextran T-2000 is used (cf. Figures 5 and 11c), as blue dextran 500_{49} has a smaller DS and therefore smaller charge density than commercial blue dextran 2000_{161}.

Conclusions

Within specific concentration ranges, aqueous mixtures of blue dextrans, undyed dextrans, and cellulose nanocrystals produce a three-phase I_1-I_2-N coexistence. To the best of our knowledge, this represents the first triphasic equilibrium of cellulose nanocrystal suspensions to exhibit two isotropic phases. The molecular weight of the dextran macromolecules appears to govern the concentrations needed to produce the I_1-I_2-N phase behavior in suspensions of electrostatically stabilized cellulose nanocrystals. Reentrant $I_2-N \rightarrow I_1-I_2-N \rightarrow I_2-N$ phase behavior as well as regions of I_2-N and I_1-N biphase coexistence are seen. For mixtures of blue dextrans with different levels of dye substitution, there exists a threshold difference in charge density above which the triphase equilibrium develops at given conditions in cellulose nanocrystal suspensions. While the interactions governing the phase equilibria are not clear, phase formation could result from the complex interplay of electrostatic and entropic forces.

Acknowledgment. The authors thank NSERC Canada and the FQRNT Quebec Centre for Self-Assembled Chemical Structures for support. We also thank Drs. Nilgun Ulkem, Greg Chauve, and Carl Bartels for their inputs.

References and Notes

(1) Zocher, H. *Z. Anorg. Allg. Chem.* **1925**, *147*, 91−110.
(2) Onsager, L. *Ann. N.Y. Acad. Sci.* **1949**, *51*, 627−659.
(3) Bawden, F. C.; Pirie, N. W. *Proc. R. Soc. London, Ser. B* **1937**, *123*, 274−320.
(4) Folda, T.; Hoffmann, H.; Chanzy, H.; Smith, P. *Nature (London)* **1988**, *333*, 55−56.
(5) Buitenhuis, J.; Donselaar, L. N.; Buining, P. A.; Stroobants, A.; Lekkerkerker, H. N. W. *J. Colloid Interface Sci.* **1995**, *175*, 46−56.
(6) Dogic, Z.; Fraden, S. *Langmuir* **2000**, *16*, 7820−7824.
(7) de Sousa Lima, M. M.; Borsali, R. *Macromol. Rapid Commun.* **2004**, *25*, 771−787.
(8) Samir, M.; Alloin, F.; Dufresne, A. *Biomacromolecules* **2005**, *6*, 612−626.
(9) Buining, P. A.; Lekkerkerker, H. N. W. *J. Phys. Chem.* **1993**, *97*, 11510−11516.
(10) Kimura, F.; Kimura, T.; Tamura, M.; Hirai, A.; Ikuno, M.; Horii, F. *Langmuir* **2005**, *21*, 2034−2037.
(11) Lekkerkerker, H. N. W.; Stroobants, A. *Nuovo Cimento* **1994**, *16D*, 949−962.
(12) Bolhuis, P. G.; Stroobants, A.; Frenkel, D.; Lekkerkerker, H. N. W. *J. Chem. Phys.* **1997**, *107*, 1551−1564.
(13) Piech, M.; Walz, J. Y. *J. Colloid Interface Sci.* **2000**, *225*, 134−146.
(14) Adams, M.; Dogic, Z.; Keller, S. L.; Fraden, S. *Nature (London)* **1998**, *393*, 349−352.
(15) Flory, P. J. *Macromolecules* **1978**, *11*, 1138−1141.
(16) Asakura, S.; Oosawa, F. *J. Chem. Phys.* **1954**, *22*, 1255−1256.
(17) Asakura, S.; Oosawa, F. *J. Polym. Sci.* **1958**, *33*, 183−192.
(18) Vrij, A. *Pure Appl. Chem.* **1976**, *48*, 471−483.
(19) Snowden, M. J.; Williams, P. A.; Garvey, M. J.; Robb, I. D. *J. Colloid Interface Sci.* **1994**, *166*, 160−167.
(20) van Bruggen, M. P. B.; Lekkerkerker, H. N. W. *Macromolecules* **2000**, *33*, 5532−5535.
(21) Dogic, Z.; Purdy, K. R.; Grelet, E.; Adams, M.; Fraden, S. *Phys. Rev. E* **2004**, *69*, 051702-1−051702-9.
(22) van der Kooij, F. M.; Vogel, M.; Lekkerkerker, H. N. W. *Phys. Rev. E* **2000**, *62*, 5397−5402.
(23) Revol, J. F.; Bradford, H.; Giasson, J.; Marchessault, R. H.; Gray, D. G. *Int. J. Biol. Macromol.* **1992**, *14*, 170−172.
(24) Revol, J. F.; Godbout, L.; Dong, X. M.; Gray, D. G.; Chanzy, H.; Maret, G. *Liq. Cryst.* **1994**, *16*, 127−134.
(25) Dong, X. M. Chiral Nematic Ordered Suspensions of Cellulose Microcrystallites. Ph.D. Thesis, McGill University, 1997.
(26) Heux, L.; Chauve, G.; Bonini, C. *Langmuir* **2000**, *16*, 8210−8212.
(27) Edgar, C. D.; Gray, D. G. *Macromolecules* **2002**, *35*, 7400−7406.
(28) Grunert, M.; Winter, W. T. *J. Polym. Environ.* **2002**, *10*, 27−30.
(29) Dong, X. M.; Kimura, T.; Revol, J. F.; Gray, D. G. *Langmuir* **1996**, *12*, 2076−2082.
(30) Dong, X. M.; Gray, D. G. *Langmuir* **1997**, *13*, 2404−2409.
(31) Dong, X. M.; Revol, J.-F.; Gray, D. G. *Cellulose* **1998**, *5*, 19−32.
(32) Araki, J.; Wada, M.; Kuga, S.; Okano, T. *Langmuir* **2000**, *16*, 2413−2415.
(33) Senti, F. R.; Hellman, N. N.; Ludwig, N. H.; Babcock, G. E.; Tobin, R.; Glass, C. A.; Lamberts, B. L. *J. Polym. Sci.* **1955**, *27*, 527−546.
(34) Ioan, C. E.; Aberle, T.; Burchard, W. *Macromolecules* **2000**, *33*, 5730−5739.
(35) Böhme, H.-J.; Kopperschläger, G.; Schulz, J.; Hofmann, E. *J. Chromatogr.* **1972**, *69*, 209−214.
(36) Beck-Candanedo, S.; Viet, D.; Gray, D. G. *Langmuir* **2006**, *22*, 8690−8695.
(37) Beck-Candanedo, S.; Viet, D.; Gray, D. G. *Cellulose* **2006**, *13*, 629−635.
(38) Sear, R. P. *J. Phys. II* **1997**, *7*, 877−886.
(39) Lekkerkerker, H. N. W.; Poon, W. C. K.; Pusey, P. N.; Stroobants, A.; Warren, P. B. *Europhys. Lett.* **1992**, *20*, 559−563.
(40) de Gennes, P. G.; Proust, J. *The Physics of Liquid Crystals*, 2nd ed.; Oxford University Press: Oxford, 1993; p 110.
(41) Sigma-Aldrich, Blue Dextran Molecular Weight 2,000,000 Product No. D5751. Product Information, 1997.
(42) Fishman, M. L.; Damert, W. C.; Phillips, J. G.; Barford, R. A. *Carbohydr. Res.* **1987**, *160*, 215−225.
(43) Nordmeier, E.; Xing, H.; Lechner, M. D. *Makromol. Chem.* **1993**, *194*, 2923−2937.
(44) Ioan, C. E.; Aberle, T.; Burchard, W. *Macromolecules* **2001**, *34*, 326−336.
(45) Hamad, E. Z.; Ijaz, W.; Ali, S. A.; Hastaoglu, M. A. *Biotechnol. Prog.* **1996**, *12*, 173−177.
(46) Poon, W. C. K.; Renth, F.; Evans, R. M. L.; Fairhurst, D. J.; Cates, M. E.; Pusey, P. N. *Phys. Rev. Lett.* **1999**, *83*, 1239−1242.

(47) Poon, W. C. K.; Renth, F.; Evans, R. M. L. *J. Phys.: Condens. Matter* **2000**, *12*, A269−A274.
(48) Renth, F.; Poon, W. C. K.; Evans, R. M. L. *Phys. Rev. E* **2001**, *64*, 031402-1−031402-9.
(49) Barois, P. In *Handbook of Liquid Crystals*; Demus, D., Goodby, J., Gray, G. W., Speiss, H. W., Eds.; Wiley-VCH: New York, 1998; Vol. 1, p 306.
(50) Moldovan, R.; Tintaru, M.; Puica, M. R.; Beica, T.; Zgura, I. *Rom. J. Phys.* **2004**, *49*, 625−630.
(51) Yu, L. J.; Saupe, A. *Phys. Rev. Lett.* **1980**, *45*, 1000−1003.
(52) Koenderink, G. H.; Vliegenthart, G. A.; Kluijtmans, S. G. J. M.; van Blaaderen, A.; Philipse, A. P.; Lekkerkerker, H. N. W. *Langmuir* **1999**, *15*, 4693−4696.
(53) Piech, M.; Walz, J. Y. *J. Colloid Interface Sci.* **2000**, *232*, 86−101.
(54) Belloni, L.; Ferreira, P. G. *Philos. Trans. R. Soc. London. A* **2001**, *359*, 867−877.
(55) Denton, A. R.; Schmidt, M. *J. Chem. Phys.* **2005**, *122*, 244911-1−244911-7.

MA0704818